

# PERIODICALLY GENERATED PROPAGATING PULSES\*

**Abstract.** Certain reaction-diffusion-convection equations with an N-shaped current-field characteristic have a solution in the form of time-periodic pulses of a field-like unknown while a current-like unknown oscillates periodically with time. A general asymptotic theory of this phenomenon, the generalized Gunn effect, has been found recently. Here we extend this theory to the case of nonlinearities having only one stable zero, which is the case for the usual Gunn effect in n-GaAs. Our ideas are presented in the context of a simple scalar model where the waves can be constructed analytically and explicit expressions for asymptotic approximations can be found.

**Key words.** Reaction-diffusion-convection equations, propagation of pulses and wavefronts, piecewise linear model, Gunn effect.

34E15, 92C30.

Date: March 23, 2022

**1. Introduction.** The Gunn effect is the periodic oscillation of the current in a passive external circuit attached to a dc-voltage biased semiconductor whose electron drift velocity has a single maximum as a function of the electric field (and therefore the curve of electron velocity versus electric field has negative slope for field values on a certain interval, a fact called *negative differential mobility*) [22, 25]. During each period of the oscillation, a pulse of the electric field is created at the injecting contact, moves through the semiconductor, and is annihilated at the receiving contact. While originally observed in bulk n-GaAs samples, similar current oscillations, mediated by pulse dynamics in dc voltage biased semiconductors, have been found in many materials, several of which lack negative differential mobility [1]. Instead, other processes (impact ionization at impurities [24], nonlinear capture coefficients [21], nonlinear recombination processes, etc) may be responsible for a current vs. local electric field characteristic curve displaying a local maximum followed by a region of negative slope (negative differential conductivity).

Propagation of pulses occurs in many systems of interest in Biology, Physics, . . . : morphogen pulses or spikes in activator-inhibitor reaction-diffusion systems modeling cell development or chemical reactors [16, 12, 13, 23], propagation of nerve impulses along myelinated or unmyelinated fibers [18, 20, 17], pulse propagation through cardiac cells [18], calcium release waves in living cells [9], semiconductor superlattices [8, 26] and oscillatory instabilities of the current in bulk semiconductors with an N-shaped current-field characteristic [1, 22, 25]. These distributed systems can be spatially discrete or continuous and can be described by a variety of model equations. Sometimes a pulse is created from an appropriate initial condition and it reaches a stable shape, moving uniformly until it arrives at a boundary. Sometimes understanding pulse dynamics is the key to describing a more complicated evolution of the system. A good example is the Gunn effect in bulk semiconductors.

While Gunn-like instabilities have been known for a long time, only recently have pulse annihilation and creation at boundaries been studied by asymptotic methods [14, 5, 6]. These theories treated the case in which the relevant nonlinear source

---

\*This research was supported by the Spanish MCyT grant BFM2002-04127-C02-01, and by the European Union under grant HPRN-CT-2002-00282. Received by the editors of SIAM J. Appl. Math. on . Manuscript number 043494-1.

<sup>†</sup>Escuela Politécnica Superior, Universidad Carlos III de Madrid, Avenida de la Universidad 30, 28911 Leganés, Spain (bonilla@ing.uc3m.es).

<sup>‡</sup>Escuela Politécnica Superior, Universidad Carlos III de Madrid, Avenida de la Universidad 30, 28911 Leganés, Spain (kinde@ing.uc3m.es).

<sup>§</sup>Departments of Mathematics and Mechanical Engineering, Stanford University, Stanford, CA 94305, USA (keller@math.stanford.edu)

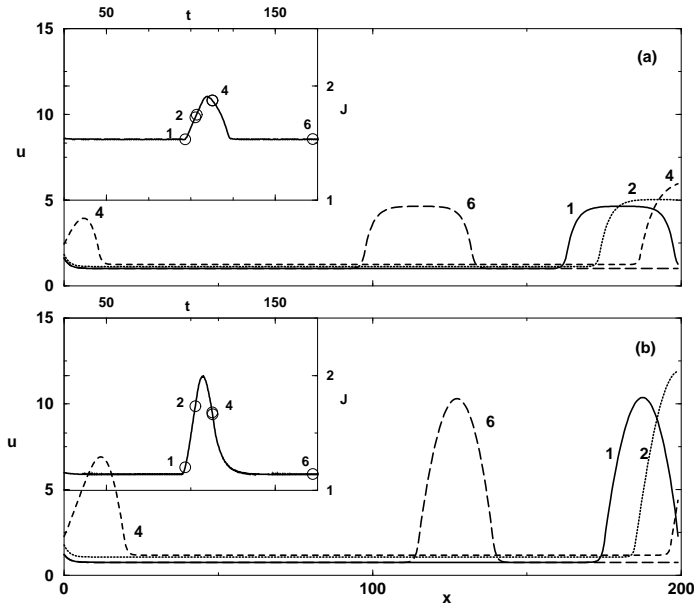


FIG. 1.1. Self-sustained oscillations of the ‘current’  $J(t)$  (see inset, which shows one period of  $J(t)$ ) mediated by pulses of the ‘field’  $u(x,t)$ , which are solutions of the model described in Section 2. The pulse profiles correspond to the times marked in the inset. Case (a): bistable source. Case (b): source with a single stable zero.

term has two stable zeros. Then there are stable wavefronts joining these two zeros, and a moving pulse is a flat region of high field bounded by two wavefronts. The pulse changes its size if its leading and trailing wavefronts move at different speeds. Fig. 1.1 shows the time-periodic oscillation of a ‘current’  $J(t)$  accompanied by the repeated generation and motion of flat-top pulses of an ‘electric field’  $u(x,t)$ , which are solutions of model equations described in Section 2. Fig. 1.1(a) corresponds to the case of a bistable nonlinear source. The asymptotic analysis of the Gunn effect is based on the dynamics of such pulses [5]. However, the source term (velocity-field characteristic curve) in very relevant materials, such as bulk n-GaAs [22], wide-miniband GaAs/AlAs superlattices [11, 15], and semi-insulating GaAs [21], does not have two stable zeros. Instead, the nonlinearity has a single stable zero, so the previous theories, based on two moving wavefronts, are not valid. Fig. 1.1(b) shows the self-sustained oscillations corresponding to this case. Can we find an asymptotic theory of pulse mediated oscillations in this case? The answer is yes, as we show in this paper.

To emphasize that our analysis applies to a class of models, we shall analyze a simpler problem than that of the Gunn effect. We will study a nonlinear reaction-diffusion-convection equation with an integral constraint [6] and a piecewise linear source term. Then the pulses can be constructed analytically, their size can change as they move, and explicit expressions for the asymptotic approximations can be found. Such a construction was used by Rinzel and Keller for the FitzHugh–Nagumo equation [20]. For Kroemer’s model, a piecewise linear electron velocity was used to calculate the exact form and speed of a steadily propagating pulse [10].

The outline of the paper is as follows. Section 2 presents our simplified model. It also reviews the key ideas of previous asymptotic theories, valid for an N-shaped nonlinearity with two stable zeros. Section 3 discusses the construction of stationary

solutions, and the kinematics of wave fronts, in the limit of long samples. When the nonlinearity is piecewise linear, the pulses can be found analytically. Section 4 discusses the dynamics of a single pulse moving from the injecting to the receiving boundary. We show that the pulse changes its form and speed adiabatically, following the instantaneous value of the current. In Section 5, we complete our description of the oscillations by explaining what happens when the pulse reaches the receiving boundary, and how a new pulse is created at the injecting boundary. Section 6 contains our conclusions. The Appendices are devoted to technical matters.

**2. Simple scalar model.** The model consists of a one-dimensional nonlinear parabolic equation for  $u(x, t)$  (the “electric field”) with an unknown forcing term  $J(t)$  (the “current”). There are also an integral constraint (the “voltage bias condition”), as well as boundary and initial conditions:

$$(2.1) \quad \frac{\partial u}{\partial t} + K \frac{\partial u}{\partial x} = \frac{\partial^2 u}{\partial x^2} + J - g(u), \quad 0 < x < L,$$

$$(2.2) \quad \frac{1}{L} \int_0^L u(x, t) dx = \phi,$$

$$(2.3) \quad u(0, t) = \rho J(t), \quad \rho > 0, \quad \frac{\partial u}{\partial x}(L, t) = 0$$

$$(2.4) \quad u(x, 0) = f(x) \geq 0, \quad 0 < x < L.$$

Here  $K$ ,  $\rho$  and  $\phi$  are positive constants.

This model becomes the Kroemer model of the Gunn effect if the advection constant  $K$  in Eq. (2.1) is replaced by  $g(u)$  [2, 3, 4, 14, 22, 25]. For the Kroemer model, existence and uniqueness of solutions have been studied by Liang [19]. Furthermore, linear stability of the stationary and moving pulse solutions have been analyzed in [3]; see also [22, 25]. A bifurcation analysis of the self-sustained oscillations due to pulse dynamics near critical values of  $\phi$  can be found in [4]. Asymptotic analyses of the Gunn effect for the Kroemer model with a bistable  $g(u)$  can be found in [14, 5].

**2.1. Bistable source  $g(u)$ .** The simplest case to consider is that of an N-shaped nonlinearity  $g(u)$  (the ‘velocity–field characteristic’) for  $u \geq 0$ , with a local maximum  $g_M = g(u_M)$ ,  $u_M > 0$ , followed by a local minimum  $g_m = g(u_m) > 0$ ,  $u_m > u_M$ . Then  $J - g(u)$  may have up to three positive zeroes for  $J > 0$ , namely  $u_1(J) < u_2(J) < u_3(J)$ . For large enough  $L$  and  $K$ ,  $g_M/u_M < \rho < g_m/u_m$ , and for  $\phi$  in a certain subinterval of  $(u_M, u_3(g_M))$ , there are stable time periodic solutions of (2.1) - (2.3) of Gunn type. As shown in Fig. 1.1(a), while  $J(t)$  oscillates periodically, pulses of  $u(x, t)$  are created at  $x = 0$ , move towards  $x = L$ , and disappear there.

The analysis of the model is simple in the asymptotic limit

$$(2.5) \quad 0 < \epsilon \equiv \frac{1}{L} \ll 1.$$

In this limit (2.1) - (2.2) may be written as

$$(2.6) \quad \frac{\partial u}{\partial s} + K \frac{\partial u}{\partial y} = \epsilon \frac{\partial^2 u}{\partial y^2} + \frac{J - g(u)}{\epsilon},$$

$$(2.7) \quad \int_0^1 u(y, s) dy = \phi,$$

where

$$(2.8) \quad y = \epsilon x, \quad s = \epsilon t.$$

Eq. (2.6) is a parabolic equation with fast reaction and slow diffusion terms. As  $\epsilon \rightarrow 0+$ ,  $u(y, s)$  is typically a piecewise constant function taking on the *order one* values  $u_1(J)$  or  $u_3(J)$  in intervals of length  $y = O(1)$ . The extrema of these intervals are typically moving internal layers. These layers are important because they bound pulses, and the self-sustained oscillation we want to describe is due to recycling and motion of pulses at the boundaries. A pulse is a region where  $u$  is  $u_3(J)$ , separated by moving wavefronts from two other regions where  $u$  is  $u_1(J)$ . There are two wavefronts bounding the pulse. In the backfront  $u$  increases from  $u_1(J)$  to  $u_3(J)$ ; this front moves with a speed  $c_+(J)$ . The forefront moves at speed  $c_-(J)$ , and in it  $u$  decreases from  $u_3(J)$  to  $u_1(J)$ . Forefront and backfront are heteroclinic trajectories connecting the two saddles  $(u_1(J), 0)$  and  $(u_3(J), 0)$  in an appropriate phase plane  $(u, du/d\chi)$ , where  $\chi = [y - Y(s)]/\epsilon$  is a moving coordinate ( $\chi = 0$  at the wavefront and  $dY/ds = c_{\pm}(J)$ ). The instantaneous value of  $J(s)$  is determined by using the integral condition (2.7). Typically  $J$  obeys the simple equation

$$(2.9) \quad \frac{dJ}{ds} = A(J) [n_+ c_+(J) - n_- c_-(J)],$$

where  $A(J) > 0$  is a known function of  $J$ , and  $n_+$  and  $n_-$  are the numbers of wavefronts with increasing and decreasing  $u$  profiles, respectively. For high-field domains,  $n_+ - n_- = 0, 1$  [6, 5]. The fixed points of Eq. (2.9) correspond to the equal area rule

$$(2.10) \quad \int_{u_1}^{u_3} [g(u) - c] du = 0$$

if  $n_+ = n_-$ , or to possible plateaus in the shape of  $J(s)$  otherwise. Many questions on the stability of the pulses and their evolution can be simply answered by analyzing Eq. (2.9) and using the asymptotic procedure explained in [6, 5]. The description of pulse creation and annihilation at the boundaries requires a finer analysis, as explained in [6, 5].

**2.2. Saturating source.** If  $g(u)$  saturates, i.e.  $g(u) \rightarrow \text{constant}$  as  $u \rightarrow \infty$ , no  $u_3(J)$  exists and the previous construction is no longer possible. What is the correct asymptotic description of a pulse in this case? Let us anticipate the answer here. As Fig. 1.1(b) shows, a pulse is a traveling wave whose profile has a single maximum, and tends to  $u = u_1(J)$  as  $x \rightarrow \pm\infty$ . The pulse is bounded by a leading front (forefront, moving at speed  $c_-$ ) and a trailing front (backfront, moving at speed  $c_+$ ). Two parameters uniquely determine the pulse: its maximum height,  $u_m$ , and the instantaneous value of  $J$ . Given  $u_m$  and  $J$ , we can find the wavefronts enclosing the pulse by simple phase plane constructions. Consider the phase plane  $(u, du/d\chi)$ ,  $\chi = x - X(t)$ , where  $X(t)$  is the instantaneous position of a wavefront and  $dX/dt$  its speed. There is a unique speed  $c_+ = c_+(J, u_m)$  for which a separatrix issuing from the saddle  $(u_1(J), 0)$  on the upper half plane reaches the  $u$  axis at  $(u_m, 0)$ . This separatrix constitutes the backfront of the pulse, and a similar construction supplies its forefront moving at speed  $c_-(J, u_m)$ . In general,  $c_+ \neq c_-$ , which implies that our pulse changes its size as it moves. How do we characterize the dynamics of pulses?

Suppose that there is a single pulse moving in the sample. We need to determine the instantaneous values of  $J$  and  $u_m$ , for they completely characterize the pulse. The pulse width,  $l$ , changes as  $dl/dt = c_- - c_+$ . On the other hand,  $l$  may be determined by a line integral on the corresponding phase plane trajectories which form the pulse. Then  $l = l(J, u_m)$ . The dc bias condition yields a connection between

$u_m$  and  $J$ ,  $u_m = U(J)$ . Then the pulse width is a function of  $J$  only,  $\varphi(J) = l(J, U(J))$ . Therefore since  $dl/ds = \varphi'(J) dJ/ds = c_- - c_+$ , we get

$$(2.11) \quad \frac{dJ}{ds} = \frac{c_+(J, U(J)) - c_-(J, U(J))}{-\varphi'(J)},$$

Typically the fixed point of this equation,  $J = J^*$ , is such that  $c_+ = c_-$  is a globally stable solution, so that  $J$  tends exponentially fast to  $J^*$ . The corresponding pulse moves steadily without changing its size. This pulse is the homoclinic orbit in the phase plane, usually given by an equal-area rule and exhaustively studied by previous authors. Notice that the present construction explains why this steadily moving pulse is stable, thereby clarifying an old issue at the heart of the Gunn effect [25, 2]. When the pulse reaches the receiving contact, a different stage of the Gunn oscillation begins. This stage and others needed to fully describe the Gunn oscillation will be explained later.

A subtle point is the following. Due to the integral condition (2.2), the pulse height and width [in the  $(y, s)$  scales] are  $O(\epsilon^{-\frac{1}{2}}) \gg 1$  and  $O(\epsilon^{\frac{1}{2}})$  respectively, while outside the pulse,  $u = u_1 = O(1)$  and  $J = O(1)$ . Thus our leading order approximation for  $u(y, s)$  is not uniformly of the same order in space. Successive approximations of a single pulse lead to the following ansatz for  $u$ :

$$u(y, s; \epsilon) \sim u^{(0)}(y, s; \epsilon) + \epsilon u^{(1)}(y, s; \epsilon).$$

Here each  $u^{(j)}(y, s; \epsilon)$  may be of different order in  $\epsilon$  for different values of the space and time variables. However we shall impose that

$$\frac{u^{(1)}}{u^{(0)}} = O(1),$$

uniformly in  $y$  and  $s$  as  $\epsilon \rightarrow 0+$ . This situation results in a changing (self-adjusting) time scale for the evolution of  $J$  described by (2.11). See Ref. [7] for the description of a similar situation in combustion theory.

**3. Boundary layers and wavefronts.** The model (2.1) - (2.4) was introduced in order to argue that the asymptotics of the Gunn effect is universal within a class of models [6]. The nonlinearity  $g(u)$  was originally N-shaped: it had three branches for  $u > 0$  (with a maximum at  $u_M > 0$  and a minimum at  $u_{\min} > u_M$  such that  $g(u_M) > g(u_{\min}) > 0$ , with  $g(u) \rightarrow \infty$  as  $u \rightarrow \infty$ ). In the present paper, we shall assume that  $g(u)$  is a smooth function having a single maximum at  $u_M > 0$ ,  $g(u_M) = g_M > 0$ , such that  $g'(0) = \beta > 0$ , and  $\lim_{u \rightarrow \infty} g(u) = \alpha \in (0, g_M)$ . To obtain explicit analytic expressions, we shall use a piecewise linear version of  $g(u)$ ,

$$(3.1) \quad g(u) = \beta u \theta(u_M - u) + \alpha \theta(u - u_M),$$

where  $\theta(x)$  is the Heaviside unit step function. See figure 3.1 where we have also shown a typical straight line  $J = u/\rho$  which gives the value of  $u$  at the left boundary. Notice that the straight line intersects  $g(u)$  at  $(u_M, \rho u_M)$ , with  $\alpha < \rho u_M < g_M$ . We want to find stable solutions  $(u(x, t), J(t))$  of Eqs. (2.1) and (2.2) under the boundary conditions (2.3) and the initial condition (2.4) for appropriate positive values of the bias  $\phi$ , in the asymptotic limit  $L \rightarrow \infty$ .

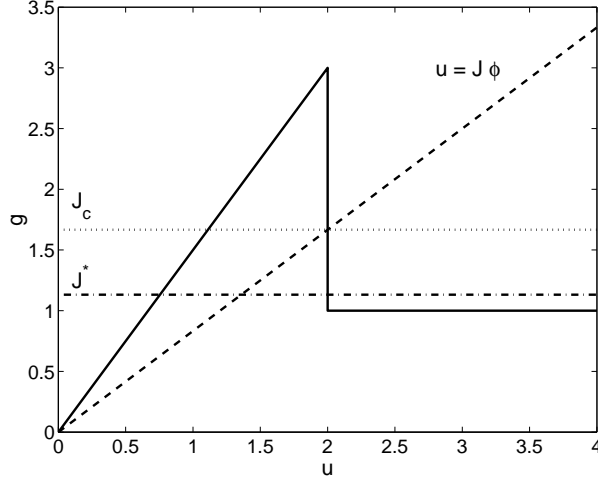


FIG. 3.1. The nonlinearity function  $g(u)$  (solid), and the curve corresponding to the boundary conditions:  $J = u/\rho$  (dashed). The parameter values are  $\phi = 1.6$ ,  $L = 200$ ,  $K = 2.0$ ,  $u_M = 2.0$ ,  $\beta = 1.5$ ,  $\alpha = 1.0$ ,  $\rho = 1.2$ .

**3.1. Outer limit and boundary layers.** If  $0 < \phi < u_M$ , there is a single stationary solution of Eqs. (2.1) - (2.3) which is easily constructed. Let  $y = x/L \equiv \epsilon x$ ,  $0 < \epsilon \ll 1$ . Introducing this scaling in Eq. (2.1) yields the leading order equation

$$(3.2) \quad J - g(u) = 0,$$

outside the boundary layers at  $y = 0, 1$ . For  $0 < J < g_M$  and  $0 < y < 1$ , (3.2) has the solutions  $u_1(J) < u_2(J)$ . Of these we may choose  $u = u_1(J)$ ,  $0 < y < 1$ , as the outer limit. Inserting it into (2.2), we find  $u_1(J) + O(\epsilon) = \phi$  and then (3.2) yields

$$(3.3) \quad J = g(\phi).$$

For the piecewise linear  $g(u)$ ,  $J = \beta \phi$ , and  $u_1(J) = J/\beta$ .

The boundary layers at  $y = 0, 1$  are solutions of the problems

$$(3.4) \quad \frac{\partial^2 U}{\partial \xi^2} \mp K \frac{\partial U}{\partial \xi} + J - g(U) = 0, \quad 0 < \xi < \infty,$$

$$(3.5) \quad U(0) = \rho J, \quad U(\infty) = u_1(J).$$

Here  $\xi = x = y/\epsilon$  for the injecting boundary layer at  $y = 0$ , and  $\xi = L - x = (1 - y)/\epsilon$  for the receiving boundary layer at  $y = 1$ . The minus (resp. plus) sign in (3.4) corresponds to the injecting (resp. receiving) boundary. Clearly the shape of the unique solution of (3.4) and (3.5) (for  $\xi = x$ ) depends on whether  $J$  is smaller or larger than  $J = J_c = u_M/\rho$ . When  $0 < J < J_c$ , the boundary layer profile monotonically decreases from  $u = \rho J$  to  $u_1 = J/\beta$ . For the piecewise linear  $g(u)$ , we have

$$(3.6) \quad U(\xi) = \frac{J}{\beta} + \left( \rho J - \frac{J}{\beta} \right) \exp \left( -\frac{\sqrt{K^2 + 4\beta} \mp K}{2} \xi \right),$$

$$(3.7) \quad \int_0^\infty (U - u_1) d\xi = \frac{2 \left( \rho J - \frac{J}{\beta} \right)}{\sqrt{K^2 + 4\beta} \mp K}.$$

However, if  $J > J_c$ , the boundary layer profile reaches a maximum before decreasing to  $u_1 = J/\beta$ . Numerical simulations show that in this case, the stationary solution of the model becomes unstable to Gunn-type oscillations. Given (3.3), this occurs for  $\phi > u_1(J_c)$ .

### 3.2. Wavefronts.

**3.2.1. Bistable source.** Let us first review how to compute the wavefronts when  $g(u)$  is N-shaped. Then (3.2) has three solutions  $u_1(J) < u_2(J) < u_3(J)$  for  $g(u_m) < J < g(u_M)$ . As explained in Ref. [6], the building blocks of the Gunn-oscillation asymptotics are wavefronts connecting  $u_1(J)$  and  $u_3(J)$ . These wavefronts adjust themselves instantaneously to the value of  $J$ , as this unknown evolves on a slower time scale (see below). A wavefront centered at  $x = X_\pm(t)$  is a monotone function of  $\chi = x - X_\pm(t)$  such that

$$\begin{aligned} u(-\infty; c_+) &= u_1(J), & u(+\infty; c_+) &= u_3(J) \quad \text{and} \\ u(-\infty; c_-) &= u_3(J), & u(+\infty; c_-) &= u_1(J). \end{aligned}$$

For the simple model used here, there is a relation between the wavefronts  $u(\chi; c_+)$  and  $u(\chi; c_-)$ :

**THEOREM 1.** *Let  $u(\chi; c_\pm)$  be the wavefront satisfying*

$$(3.8) \quad \frac{d^2 u}{d\chi^2} - (K - c_\pm) \frac{du}{d\chi} + J - g(u) = 0,$$

$$(3.9) \quad u(-\infty; c_+) = u_1(J), \quad u(+\infty; c_+) = u_3(J),$$

$$(3.10) \quad u(-\infty; c_-) = u_3(J), \quad u(+\infty; c_-) = u_1(J),$$

where  $\chi = x - X_\pm(t)$  ( $X_\pm$  is the position of the front at time  $t$ , determined by imposing  $u(0) = u^0$ .  $dX_\pm/dt = c_\pm$ ). Then we have

$$(3.11) \quad u(\chi; c_-) = u(-\chi; c_+), \quad c_+ + c_- = 2K.$$

The proof is evident. This theorem shows that we only need to construct  $u(\chi; c_+)$  and find  $c_+$  in order to have  $u(\chi; c_-)$  and  $c_-$ .

**3.2.2. Saturating source.** Let now  $g(u)$  be a function with only two branches such as (3.1). A wavefront is the only monotone trajectory connecting  $(u_1(J), 0)$  and a given point on the  $u$  axis  $(u_m, 0)$ . There is again a symmetry result for these wavefronts:

**THEOREM 2.** *Let  $u(\chi; c_+)$  be the wavefront satisfying (3.8),  $\partial u / \partial \chi > 0$  for  $-\infty < \chi \equiv x - X_+(t) < \chi_m$ , and*

$$(3.12) \quad \begin{aligned} u(-\infty; c_+) &= u_1(J), & u(0; c_+) &= u^0, \\ u(\chi_m; c_+) &= u_m, & \frac{\partial u}{\partial \chi}(\chi_m; c_+) &= 0. \end{aligned}$$

Here  $dX_+/dt = c_+$ , and  $2\chi_m = l(J, u_m) > 0$  is a function of  $J$  and  $u_m$ . Then the wavefront satisfying (3.8),  $\partial u / \partial \chi < 0$  for  $-\chi_m < \chi \equiv x - X_-(t) < \infty$ ,  $c_- = dX_-/dt$ , and

$$(3.13) \quad \begin{aligned} u(-\chi_m; c_-) &= u_m, & \frac{\partial u}{\partial \chi}(-\chi_m; c_-) &= 0, \\ u(0; c_-) &= u^0, & u(+\infty; c_-) &= u_1(J), \end{aligned}$$

is such that (3.11) holds.

Again the proof is immediate.

Let us now choose a certain  $u_m = U(J)$  for each  $\phi > u_M$  so that the bias condition (2.2) holds for a pulse made out of:

- a backfront  $u(\chi; c_+)$  at  $x = X_+(t)$ ,  $\chi = x - X_+(t)$ ; and
- a forefront  $u(-\chi; c_+)$  at  $X_- = X_+ + 2\chi_m$ . Now  $\chi = x - X_-(t)$ .

The pulse  $u(\chi; c_+)$  can be constructed explicitly for the piecewise linear  $g(u)$  of (3.1). If we choose  $u^0 = u_M$ , the solution of Eqs. (3.8) and (3.9) which is continuous and has a continuous first derivative at  $\chi = 0$  is

$$(3.14) \quad u(\chi; c_+) = u_1(J) + [u_M - u_1(J)] e^{\lambda_+ \chi} \quad \chi < 0,$$

$$(3.15) \quad u(\chi; c_+) = u_M + \frac{J - \alpha}{K - c_+} \chi + B_+ \left[ e^{(K - c_+) \chi} - 1 \right] \quad \chi > 0.$$

Here  $u_1(J) = J/\beta$ , and

$$(3.16) \quad \lambda_+ = \frac{K - c_+}{2} + \sqrt{\left( \frac{K - c_+}{2} \right)^2 + \beta},$$

$$(3.17) \quad B_+ = \frac{1}{K - c_+} \left[ \lambda_+ [u_M - u_1(J)] - \frac{J - \alpha}{K - c_+} \right],$$

$$(3.18) \quad \begin{aligned} \chi_m &= \frac{1}{K - c_+} \ln \left[ -\frac{J - \alpha}{(K - c_+)^2 B_+} \right] \\ &= -\frac{1}{K - c_+} \ln \left[ 1 - \frac{\lambda_+ (u_M - u_1)(K - c_+)}{J - \alpha} \right], \end{aligned}$$

$$(3.19) \quad u_m = u_M + \frac{J - \alpha}{K - c_+} \chi_m + B_+ \left[ e^{(K - c_+) \chi_m} - 1 \right].$$

If these expressions are inserted in the bias condition (2.2),  $c_+$ ,  $\chi_m$  and  $u_m$  may be determined as functions of  $J$  for a fixed  $\phi$ . Figures 3.2 and 3.3 show the phase planes and the trajectories corresponding to  $u(\chi; c_+)$  and  $u(\chi; c_-)$ , respectively, for a given value of  $J = 1.3$ . Fig. 4.1 shows  $\chi_m$  and  $u_m$  as functions of  $J$ .

There are two important approximations to the wavefronts of Theorem 2, which yield either approximately triangular pulses ( $c_+ \neq c_-$ ,  $u_m \gg 1$ ) or the homoclinic pulse ( $c_+ = c_- = K$ ). These two limiting cases are described in detail in Appendix A.

#### 4. Pulse Dynamics.

**4.1. One pulse far from the boundaries.** Let us consider a single pulse moving far from the boundaries, as described in the previous Section. Its height and width are established by imposing the integral condition (2.2). The result will show that the pulse is a tall and narrow moving layer which changes size as it moves. At certain stages of the periodic Gunn oscillation (see below), the pulse height is  $u = O(\epsilon^{-\frac{1}{2}})$ , its width is  $\Delta y = O(\epsilon^{\frac{1}{2}})$ , so that the pulse excess area (in  $y$  space units) is  $O(1)$ . The inner core of the pulse contributes an order 1 amount to the bias whereas its exponential tails approaching  $u_1(J)$  yield an  $O(\epsilon)$  correction to its excess area. Thus we suggest a decomposition of the solution  $u$  into an outer solution valid outside the pulse and boundary layers, and inner solutions comprising the front(s) and boundary layers. In this Section, we shall calculate the leading order term in each asymptotic expansion explicitly. The first correction to these results can be found in Appendix B.



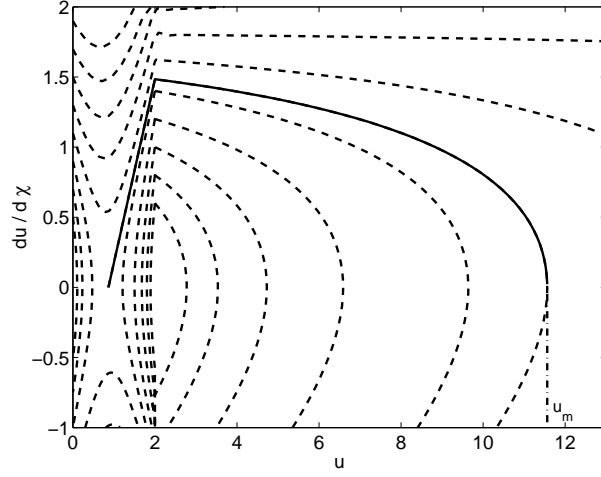


FIG. 3.2. Phase plane  $(u, du/d\chi)$  and trajectory corresponding to  $u(\chi; c_+)$  for  $J = 1.3$ ,  $c_+ = 1.8359$ . Other parameter values as in Figure 3.1.

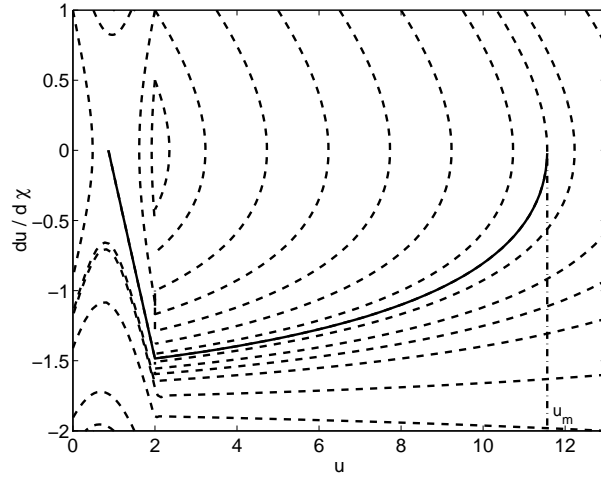


FIG. 3.3. Phase plane  $(u, du/d\chi)$  and trajectory corresponding to  $u(\chi; c_-)$  for  $J = 1.3$ ,  $c_- = 2.1641$ . Other parameter values as in Figure 3.1.

**4.1.1. Outer solution.** The outer solution is

$$(4.1) \quad u^{outer} = u^{(0)}(y, s) + \epsilon u^{(1)}(y, s) + O(\epsilon^2)$$

$$(4.2) \quad J = J^{(0)}(s) + \epsilon J^{(1)}(s) + O(\epsilon^2).$$

Here  $u^{(0)} = O(1)$  yields an order 1 contribution to the integral condition (2.2), of the same order as that provided by integration of the excess area of the pulse inner core.  $\epsilon u^{(1)}$  yields an order  $\epsilon$  contribution to (2.2), of the same order as that provided by integration of the excess area of the pulse tails. Inserting this Ansatz into (2.6), we

obtain

$$(4.3) \quad J^{(0)} - g(u^{(0)}) = 0,$$

$$(4.4) \quad J^{(1)} - g'(u^{(0)}) u^{(1)} = \frac{\partial u^{(0)}}{\partial s} + K \frac{\partial u^{(0)}}{\partial y}.$$

Solving (4.3) and (4.4) yields

$$(4.5) \quad u^{(0)} = u_1(J^{(0)}) = \frac{J^{(0)}}{\beta},$$

$$(4.6) \quad u^{(1)} = \frac{J^{(1)} - \frac{1}{g'_1} \frac{dJ^{(0)}}{ds}}{g'_1} = \frac{1}{\beta} \left( J^{(1)} - \frac{1}{\beta} \frac{dJ^{(0)}}{ds} \right).$$

$J^{(0)}$  and  $J^{(1)}$  will be found later from the integral constraint.

**4.1.2. Two-term description of the pulse.** The pulse described in the previous Section may be considered a moving inner layer solution. Its height is much larger than 1 and its width much smaller than 1 (the precise orders will be determined later). We shall assume

$$(4.7) \quad u^{inner} \sim P^{(0)}(y, s; \epsilon) + \epsilon P^{(1)}(y, s; \epsilon),$$

where  $P^{(0)}$  is the pulse solution of (3.8) described in Theorem 2:

$$(4.8) \quad \begin{aligned} P^{(0)}(y, s; \epsilon) = & u(x - X_+; c_+) \theta[\chi_m - (x - X_+)] \\ & + u(X_+ + 2\chi_m - x; c_+) \theta[x - X_+ - \chi_m]. \end{aligned}$$

$P^{(0)}(y, s; \epsilon)$  and  $P^{(1)}(y, s; \epsilon)$  depend on  $\epsilon$  in such a way that

$$\frac{P^{(1)}(y, s; \epsilon)}{P^{(0)}(y, s; \epsilon)} = O(1), \quad \text{as} \quad \epsilon \rightarrow 0+$$

uniformly in  $y, s$ . The inner expansion (4.7) is chosen so that the pulse inner core in  $P^{(0)}$  yields an order 1 contribution to the bias condition whereas its tails together with the inner core of  $\epsilon P^{(1)}$  yield an  $O(\epsilon)$  contribution. The latter is of the same order as the contribution of the outer solution,  $\epsilon u^{(1)}$ , to the bias.

In Eq. (4.8), the location of the fronts and their velocities are:

$$(4.9) \quad \begin{aligned} X_+ & \sim X_+^{(0)}(t) + \epsilon X_+^{(1)}(t), \\ c_+ & \sim c_+^{(0)} + \epsilon c_+^{(1)}, \end{aligned}$$

and similarly for  $X_-$  and  $c_-$ . Inserting (4.2) and (4.7) - (4.9) in (2.1) and (3.9), we obtain for the trailing front

$$(4.10) \quad \frac{\partial^2 P^{(0)}}{\partial \chi^2} - (K - c_{\pm}^{(0)}) \frac{\partial P^{(0)}}{\partial \chi} + J^{(0)} - g(P^{(0)}) = 0,$$

$$(4.11) \quad \begin{aligned} P^{(0)}(-\infty; c_+^{(0)}) &= u^{(0)} = u_1, \quad P^{(0)}(0; c_+^{(0)}) = u_M, \\ P^{(0)}(\chi_m; c_+^{(0)}) &= u_m, \quad \frac{\partial P^{(0)}}{\partial \chi}(\chi_m; c_+^{(0)}) = 0, \end{aligned}$$

whose solution is (4.8), and

$$(4.12) \quad \frac{\partial^2 P^{(1)}}{\partial \chi^2} - (K - c_{\pm}^{(0)}) \frac{\partial P^{(1)}}{\partial \chi} - g'(P^{(0)})P^{(1)} = \frac{\partial P^{(0)}}{\partial s} - J^{(1)} - c_{\pm}^{(1)} \frac{\partial P^{(0)}}{\partial \chi},$$

$$(4.13) \quad P^{(1)}(-\infty; c_+^{(0)}) = u^{(1)}, \quad \frac{\partial P^{(1)}}{\partial \chi}(\chi_m; c_+^{(0)}) = 0.$$

The leading front of the pulse obeys similar expressions. The correction  $P^{(1)}$  is calculated in Appendix B, in which explicit formulas for piecewise linear  $g(u)$  are given.

**4.2. General equation for  $J^{(0)}$ .** Using Theorem 2, we can calculate the bias condition for a single pulse moving far from the boundaries as

$$(4.14) \quad \begin{aligned} \phi = & u_1(J^{(0)}) + 2\epsilon \int_0^{\chi_m} (P^{(0)} - u_1) d\chi \\ & + 2\epsilon \int_{-\infty}^0 (P^{(0)} - u_1) d\chi + \epsilon \frac{J^{(1)} - g'_1 J_s^{(0)}}{g_1'^2} \\ & + 2\epsilon^2 \int_0^{\chi_m} \left( P^{(1)} - \frac{J^{(1)} - g'_1 J_s^{(0)}}{g_1'^2} \right) d\chi \\ & + \epsilon \int_0^\infty [U_L(\xi) - u_1] d\xi \\ & + \epsilon \int_0^\infty [U_R(\xi) - u_1] d\xi + O(\epsilon^2). \end{aligned}$$

Here the bias is the sum of the areas of the regions inside and outside the moving pulse. The leading order contributions to these areas are the first two terms on the right side, which are of order 1. They are: (i) the leading order contribution of the outer solution and (ii) the leading order contribution of the inner core of the pulse. The other terms are  $O(\epsilon)$  and correspond to:

- (i) the tails of the pulse to leading order,

$$2\epsilon \int_{-\infty}^0 (P^{(0)} - u_1) d\chi = \frac{2\epsilon(u_M - u_1)}{\lambda_+},$$

- (ii) the second order contribution to the outer solution,
- (iii) the second order contribution to the area of the inner core of the pulse,  $2\epsilon^2 \int_0^{\chi_m} P^{(1)} d\chi = O(\epsilon)$  (we have ignored a much smaller term of order  $\epsilon^2 \chi_m$ ),
- (iv) the layer at the left boundary, Eqs. (3.6) and (3.7):

$$\epsilon \int_0^\infty (U_L - u_1) d\xi = \frac{2\epsilon(\rho - \beta^{-1}) J^{(0)}}{\sqrt{K^2 + 4\beta} - K},$$

The area of the injecting (left) boundary layer becomes of order 1 when a new pulse is being shed; otherwise it is of order  $\epsilon$ , as indicated above.

If the pulse is far from the boundaries only the first two terms are of order 1, and we have

$$\begin{aligned}
 \phi &= u_1(J^{(0)}) + 2\epsilon \left[ \chi_m(u_M - u_1 - B_+) \right. \\
 &\quad \left. + \frac{(J^{(0)} - \alpha)\chi_m^2}{2(K - c_+^{(0)})} + \frac{B_+ \left( e^{(K - c_+^{(0)})\chi_m} - 1 \right)}{K - c_+^{(0)}} \right] + O(\epsilon) \\
 &= u_1 + 2\epsilon \left[ \chi_m(u_M - u_1 - B_+) + \frac{(J^{(0)} - \alpha)\chi_m^2}{2(K - c_+^{(0)})} \right. \\
 (4.15) \quad &\quad \left. + \frac{B_+ \lambda_+(u_M - u_1)}{J^{(0)} - \alpha} \right] + O(\epsilon).
 \end{aligned}$$

Now we can proceed as sketched in Section 2. Eq. (3.18) allows us to obtain  $c_+^{(0)}$  as a function of  $J^{(0)}$  and  $\chi_m$ :

$$(4.16) \quad c_+^{(0)} = \Xi(J^{(0)}, \chi_m),$$

for a fixed value of  $\phi$ . Inserting this function in (4.15), we can determine  $\chi_m$  as a function of  $J^{(0)}$ . Then (3.19) yields  $u_m$  as a function of  $J^{(0)}$ . The results are certain functions:

$$(4.17) \quad \chi_m = \frac{\varphi(J^{(0)})}{2}, \quad u_m = U(J^{(0)}),$$

that have been depicted in Fig. 4.1. Time differentiation of  $2\chi_m = \varphi(J^{(0)})$  yields Eq. (2.11):

$$(4.18) \quad \frac{dJ^{(0)}}{ds} = 2 \frac{c_+^{(0)}(J^{(0)}, U(J^{(0)})) - K}{-\varphi'(J^{(0)})},$$

which describes the time evolution of  $J^{(0)}$ . Provided that  $J^{(0)}(0) > J^*$ ,  $J^{(0)}$  decreases exponentially fast to  $J^*$  such that  $c_+^{(0)} = c_-^{(0)} = K$ . The pulse then moves at constant  $J^{(0)} = J^*$  and speed  $K$ , and it is a homoclinic orbit of the phase plane (3.8) with  $c = K$ , as shown in Fig. 4.2.

Figure 4.3 compares the leading order asymptotic solution with the numerical solution. The upper part shows the time evolution of  $J(t)$  and the lower part  $u(x, t)$  at the times marked in the upper figure. Notice that initially  $J(t)$  decreases exponentially fast to  $J^*$ . Consider an instant (point 6) at which the wave is fully developed and far from the boundaries. We observe that the profile of the asymptotic solution has a larger height and is slightly thinner than the numerical solution. Why? We have neglected  $O(\epsilon)$  terms (boundary layers, wave tails, ...) when calculating the integral condition with the leading order asymptotic solution. Then  $J^{(0)}(t)$  is slightly larger than the numerically calculated  $J(t)$ . The asymptotic profile fully agrees with the homoclinic solution described in Appendix A by (A.10), (A.11) and (A.12) (also calculated excluding order  $\epsilon$  effects).

The previous ideas are correct if we can show that  $J^{(0)}$  evolves on a slow time scale, say  $\sigma = \sqrt{\epsilon}(t - t_0)$  or  $\tau = \epsilon(t - t_0)$ . To see this we should analyze (4.15) and the previous equations with a little more care. We shall show that there are two limiting cases for which the pulse can be easily calculated and (2.11) explicitly obtained to leading order:

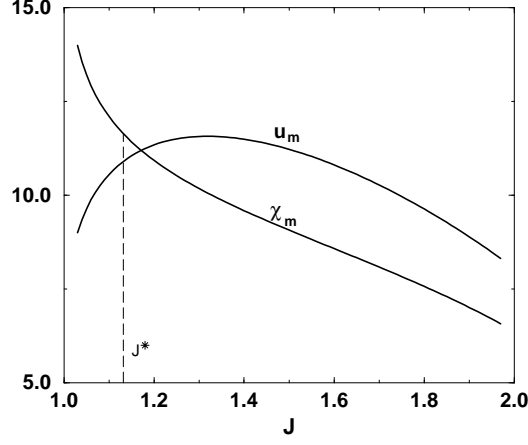


FIG. 4.1. Half-width  $\chi_m$  and maximum height  $u_m$  of the single pulse as a function of  $J$  for the same parameter values as in Figures 3.1 to 3.3

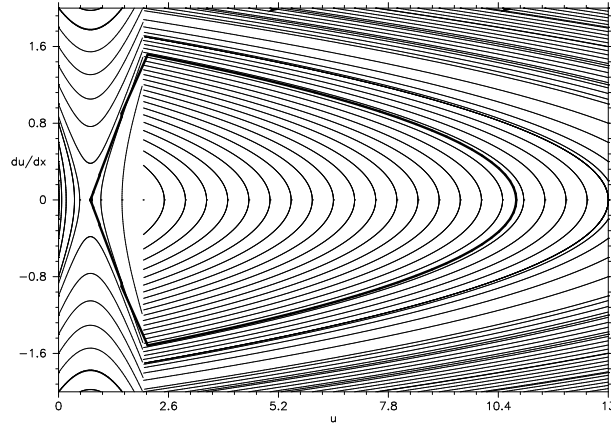


FIG. 4.2. Phase plane  $(u, du/d\chi)$  and homoclinic orbit for  $J^* = 1.13182$ ,  $c = 2$ . Other parameter values are as in Figure 3.1.

- $J^{(0)} - J^* = O(1)$ ,  $K - c_+^{(0)} = O(1)$  and  $(J^{(0)} - \alpha)\chi_m \gg 1$ . The limiting pulse is a triangular wave formed by pieces of phase plane trajectories which do not tend exponentially to infinity as  $\chi \rightarrow \pm\infty$ .
- $(K - c_+^{(0)}) \ll (J^{(0)} - \alpha) \ll 1$ ,  $\chi_m \gg 1$ . The limiting pulse is the homoclinic trajectory with  $c = K$ .

In the first case,  $J^{(0)}$  evolves on the slow time scale  $\sigma = \sqrt{\epsilon}(t - t_0)$ . In the second case, the time over which  $J^{(0)}$  varies appreciably is  $o(\epsilon^{-1})$ . One period of the Gunn oscillation contains stages during which these limiting cases are good approximations to (2.11). In fact the Gunn oscillation may be considered as transitions from one limiting case to the other depending on the number of pulses existing at the time. Then  $J^{(0)}$  changes slowly with time which justifies our wavefront constructions.

Appendix C analyzes the dynamics of pulses corresponding to the two limiting cases of triangular and homoclinic pulses. At this point, we may call attention to two

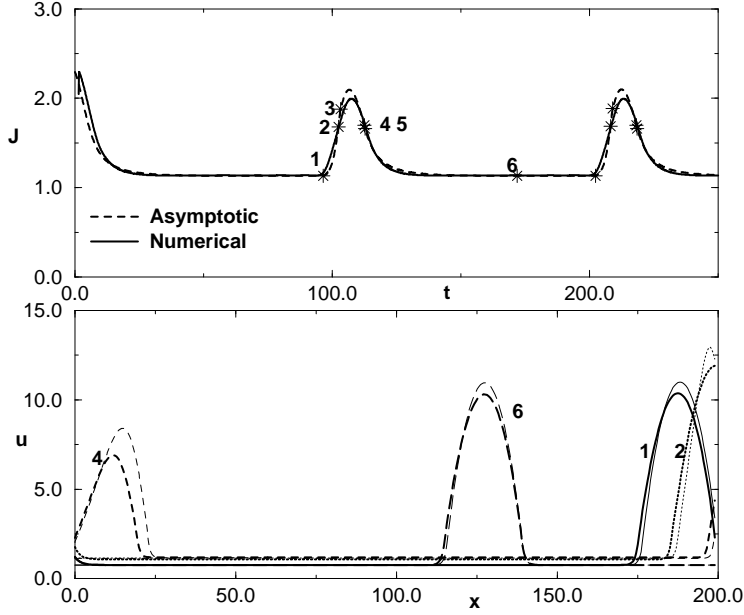


FIG. 4.3. Upper: time evolution of  $J$ . Times marked correspond to; (1) wave reaches receiving contact, (2)  $J$  reaches  $J_c$  (3)  $\chi_m < \chi_L$  (4) wave completely exits (5)  $J < J_c$  (6) fully developed wave. Lower: profiles of  $u(x, t)$  at the times marked in the upper figure.

peculiar features of our results:

1. Our leading-order approximation for the solution is of order one outside a pulse, but it is much larger inside it: of order  $\epsilon^{-\frac{1}{2}}$ .
2. The proper time scale for the variation of  $J$  is  $\epsilon^{\frac{1}{2}}t$  if the pulse may be approximated by a triangular wave. It is slower as the pulse approaches a homoclinic pulse. Both these approximations are limits of the same equation, (2.11). Thus this equation contains more than one asymptotic limit and its time scale is changing as time changes.

**5. Pulse dynamics near the boundaries.** In the previous Section, we described the dynamics of a single pulse far from the boundaries. Basically the pulse approaches the homoclinic pulse on a slow time scale: at each time on the scale  $t$  the pulse follows adiabatically the instantaneous value of  $J$ .  $J$  changes on the scale  $\sigma = \sqrt{\epsilon}t$  or even more slowly as described by Eq. (2.11), where  $\varphi$  is a function of  $J$  and  $\epsilon$  ( $\varphi(J)$  is of order  $\epsilon^{-\frac{1}{2}}$  or larger). In this Section we shall describe what occurs when the pulse reaches the receiving boundary at  $x = L$  and beyond, until a period of the Gunn oscillation is completed.

**5.1. Pulse disappearing through the receiving boundary.** Let us assume that a single pulse has reached its asymptotic shape ( $J^{(0)} = J^*$ ) and it advances with speed  $K$  until its forefront reaches  $X_- = L$  at time  $t_1$ . Afterwards, it begins leaving the sample. As time elapses the wave *exits* through the receiving boundary and therefore the area under the wave decreases. Since the total area has to satisfy the bias condition, this loss of area has to be compensated by a corresponding increase in  $u_1$  so that equation (2.2) still holds.

Let us denote by  $u_L$  the value of the pulse inner solution  $P^{(0)}(y, s)$  at the receiving

boundary.  $u_L$  is obtained from equation (3.15) for  $u(x - X_-^{(0)}; c_+^{(0)}) = u(X_-^{(0)} - x; c_+^{(0)}) = u(2\chi_m - \chi; c_+^{(0)})$  when  $\chi - 2\chi_m = L - X_-^{(0)}$ . The corresponding argument of  $u(X_-^{(0)} - x; c_+^{(0)})$  is  $\chi_L = X_-^{(0)} - L > 0$ . When  $0 < \chi_L < \chi_m$ , the bias condition (2.2) yields

$$(5.1) \quad \begin{aligned} \phi &= u_1 + \Phi^{(0)}(J, c_+^{(0)}, \chi_m, \chi_L) + \epsilon \Phi^{(1)}(J, c_+^{(0)}, \chi_m, \chi_L, J^{(1)}) + O(\epsilon^2), \\ \frac{\Phi^{(0)}(J, c_+^{(0)}, \chi_m, \chi_L)}{\epsilon} &= 2 \int_0^{\chi_m} [u(\chi; c_+^{(0)}) - u_1] d\chi - \int_0^{\chi_L} [u(\chi; c_+^{(0)}) - u_1] d\chi \\ &= (2\chi_m - \chi_L)(u_M - u_1 - B_+) + \frac{(J - \alpha)}{(K - c_+^{(0)})} \left( \chi_m^2 - \frac{\chi_L^2}{2} \right) \\ &\quad + \frac{B_+ \left( 2e^{(K - c_+^{(0)})\chi_m} - e^{(K - c_+^{(0)})\chi_L} - 1 \right)}{K - c_+^{(0)}}, \end{aligned} \quad (5.2)$$

$$(5.3) \quad \begin{aligned} \Phi^{(1)}(J, c_+^{(0)}, \chi_m, \chi_L, J^{(1)}) &= \int_{-\infty}^0 (P^{(0)} - u_1) d\chi + \frac{J^{(1)} - g'_1 J_s^{(0)}}{g_1'^2} \\ &\quad + 2\epsilon \int_0^{\chi_m} P^{(1)} d\chi - \epsilon \int_0^{\chi_L} P^{(1)} d\chi + \epsilon \int_0^\infty [U_L(\xi) - u_1] d\xi, \end{aligned}$$

instead of (4.14). In this equation  $\Phi^{(0)}$  and  $\Phi^{(1)}$  are of order 1 because the integrations of  $P^{(0)}$  and  $P^{(1)}$  over the inner core of the pulse are of order  $\epsilon^{-1}$ . Eq. (5.1) yields

$$(5.4) \quad \phi = u_1 + \Phi^{(0)}(J^{(0)}, c_+^{(0)}, \chi_m, \chi_L),$$

$$(5.5) \quad \Phi^{(1)}(J^{(0)}, c_+^{(0)}, \chi_L, \chi_m, J^{(1)}) = 0.$$

We shall now find the evolution equation for  $J^{(0)}$  by a procedure similar to that used to find (4.18). The right side of (5.4) depends on  $J^{(0)}$ ,  $c_+^{(0)}$ ,  $\chi_m$  and  $\chi_L$ .  $\chi_m$  is a function of  $J^{(0)}$  and  $c_+^{(0)}$  given by (3.18). As wavefront velocity  $c_+^{(0)}$ , we shall use the function of  $J^{(0)}$  (for a fixed value of  $\phi$ ) that was determined at the end of Section 3. Then the right side of (5.4) is a function of  $J^{(0)}$  and  $\chi_L$  only (for fixed  $\phi$ ):

$$(5.6) \quad \begin{aligned} \phi &= \mathcal{B}(J^{(0)}, \chi_L) \equiv u_1(J^{(0)}) \\ &\quad + \Phi^{(0)}(J^{(0)}, c_+^{(0)}(J^{(0)}), \chi_m(J^{(0)}, c_+^{(0)}(J^{(0)})), \chi_L). \end{aligned}$$

$\chi_L$  can be explicitly calculated from

$$(5.7) \quad \frac{d\chi_L}{dt} = c_-^{(0)} = 2K - c_+^{(0)}, \quad \chi_L(t_1) = 0,$$

where  $c_+^{(0)}$  is our known function of  $J^{(0)}$ . We can obtain a closed system of equations for  $\chi_L$  and  $J^{(0)}$  by differentiating (5.6) with respect to time and then using (5.7). The result is

$$(5.8) \quad \frac{\partial \mathcal{B}}{\partial J^{(0)}} \frac{dJ^{(0)}}{dt} \sim \epsilon (u_L - u_1) (2K - c_+^{(0)}).$$

Here we have used that (5.2) and (5.6) imply  $\partial \mathcal{B} / \partial \chi_L = -(u_L - u_1)$ .

The time evolution of  $J^{(0)}$  is found by solving this equation while the wave disappears through the receiving contact. Having found the solution to leading order,

(5.5) yields the correction  $J^{(1)}$ . Numerical solution of (5.1) to (5.8) shows that  $J^{(0)}$  increases with time, as shown in the region between times 1 and 2 in figure 4.3. Notice that this increase agrees with the numerical solution of (2.1-2.4).

Depending on the bias  $\phi$ , one of the following two events may happen first:

- (i)  $J^{(0)}$  reaches  $J_c$ , or
- (ii)  $\chi_L = \chi_m$ .

In both cases the stage described by the previous equations ends. In case (i), a new wave is created at  $x = 0$ , whereas in case (ii) (5.1) should be changed to

$$(5.9) \quad \phi = u_1 + \Psi^{(0)}(J^{(0)}, c_+^{(0)}, \chi_L) + \epsilon \Psi^{(1)}(J^{(0)}, c_+^{(0)}, \chi_L, J^{(1)}) + O(\epsilon^2),$$

$$\Psi^{(0)}(J^{(0)}, c_+^{(0)}, \chi_L) = \epsilon \int_0^{\chi_L} [u(\chi; c_+^{(0)}) - u_1] d\chi$$

$$(5.10) \quad = \epsilon \left[ \frac{(J^{(0)} - \alpha)\chi_L^2}{2(K - c_+^{(0)})} + \chi_L(u_M - u_1 - B_+) + \frac{B_+ (e^{(K - c_+^{(0)})\chi_L} - 1)}{K - c_+^{(0)}} \right],$$

$$(5.11) \quad \Psi^{(1)}(J, c_+^{(0)}, \chi_L, J^{(1)}) = \int_{-\infty}^0 [u(\chi; c_+^{(0)}) - u_1] d\chi + \frac{J^{(1)} - g_1' J_s^{(0)}}{g_1'^2}$$

$$+ \epsilon \int_0^{\chi_L} P^{(1)} d\chi + \epsilon \int_0^\infty [U_L(\xi) - u_1] d\xi,$$

where now  $\chi_L = L - X_+^{(0)} > 0$  and

$$(5.12) \quad \frac{d\chi_L}{dt} = -c_+^{(0)}, \quad \chi_L(t_2) = \chi_m(t_2).$$

Here  $t_2$  is the time at which the maximum of the pulse reaches  $x = L$  (equivalently  $\chi_L = \chi_m$  in the previous stage). Similar arguments to those used in the previous stage lead to,

$$(5.13) \quad \left( \frac{1}{\beta} + \frac{\partial \tilde{\Psi}^{(0)}}{\partial J^{(0)}} \right) \frac{dJ^{(0)}}{dt} \sim \epsilon (u_L - u_1) c_+^{(0)},$$

where  $\tilde{\Psi}^{(0)}(J^{(0)}, \chi_L) = \Psi^{(0)}(J^{(0)}, c_+^{(0)}(J^{(0)}), \chi_L)$ .

This stage lasts until  $J^{(0)}$  reaches  $J_c$  and a new pulse is shed. If the bias is small enough, the solution of these equations may be such that  $J^{(0)}$  never reaches  $J_c$  and it eventually decreases with time. In such case, the pulse exits and leaves a stable stationary state in its wake after  $\chi_L = 0$ . Notice that setting  $\chi_L = \chi_m = 0$  in (3.18) implies a front velocity (A.7). Thus the velocity of the disappearing wavefront approaches that of the triangular wave, although the shapes of the respective wavefronts may differ greatly. As in the previous stage, we find  $J^{(1)}$  by solving the equation  $\Psi^{(1)}(J^{(0)}, c_+^{(0)}, \chi_L, J^{(1)}) = 0$ .

**5.2. Pulse shedding at the injecting boundary.** If  $J(t)$  reaches  $J_c$  at  $t = t_2$ , the boundary layer becomes unstable and a new pulse starts being shed at the injecting boundary. The boundary layer profile,  $U(x, t)$  solves the following semiinfinite integrodifferential problem:

$$(5.14) \quad \frac{\partial U}{\partial \sigma} + K \frac{\partial U}{\partial x} - \frac{\partial^2 U}{\partial x^2} + g(U) = J(\sigma),$$

$$(5.15) \quad U(0, \sigma) = \rho J,$$



whose solution exhibits an explosion-type behavior and a rapid growth of the area enclosed by the boundary layer which can no longer be neglected. This increase in area is to be compared with the area released by the disappearing pulse at  $x = L$ . Initially, the area released is larger and this net area loss has to be compensated by an equal increase in the area of the outer solution, so that  $J$  continues to increase although at a slower rate. After a short time, the growth of the boundary layer is larger than the area released, so that  $J$  reaches a maximum and starts decreasing.

The structure of the injecting boundary layer when  $J > J_c$  is as follows:

1.  $u = u(x; J, U_m)$  is quasi-stationary for  $0 < x < X_m$  such that (3.4) holds with  $u(0; J, U_m) = \rho J$ ,  $u(X_m; J, U_m) = U_m$ , with  $\partial u(X_m; J, U_m)/\partial x = 0$ . The boundary layer solution is the trajectory of the phase plane corresponding to (3.4) which leaves the vertical line  $u = \rho J$  at  $x = 0$  and intersects the  $u$  axis at  $u = U_m$ . Notice that this trajectory is uniquely determined by giving  $J$  and  $U_m$ .
2. For  $x > X_m$ , the boundary layer is a wavefront of type  $u(\chi; c_-)$  moving at speed  $C_-$ . This speed and the forefront are uniquely determined by  $J$  and  $U_m$ :  $u = u(\xi; C_+)$ ,  $\xi = X_m - x$ , with  $C_+ = 2K - C_-$ ,  $u(-\infty; C_+) = u_1(J)$ ,  $u(0; C_+) = U_m$ ,  $u(\xi_m; C_+) = U_m$ ,  $\partial u(\xi_m; C_+)/\partial \xi = 0$ .

The bias condition (including the injecting boundary layer) is

$$(5.16) \quad \phi = u_1 + \tilde{\Psi}^{(0)}(J, \chi_m, \chi_L) + \epsilon A^{(0)}(t) + O(\epsilon),$$

$$(5.17) \quad A^{(0)} = \int_0^\infty [U(\xi) - U_\infty] d\xi,$$

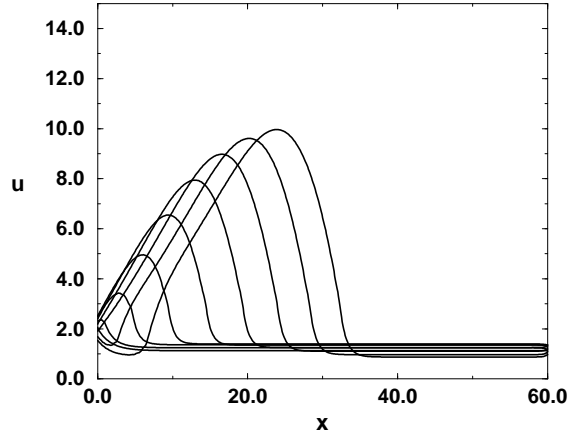
provided that the maximum of the old pulse has leaved the sample. Time differentiation of (5.16) yields

$$(5.18) \quad \left( \frac{1}{\beta} + \frac{\partial \tilde{\Psi}^{(0)}}{\partial J^{(0)}} \right) \frac{dJ^{(0)}}{dt} \sim -\epsilon \frac{dA^{(0)}}{dt} + \epsilon (u_L - u_1) c_+^{(0)}.$$

Equations (5.12), (5.16), and (5.18), together with (5.2), (5.10) and (4.17), constitute a closed system of equations for the unknowns  $J$ ,  $\chi_L$ , and  $\chi_m$ . During this stage,  $J$  initially increases and then decreases until it either reaches again  $J_c$ , or the old wave completely disappears. In the latter case, the evolution of  $J(t)$  is still given by equation (5.18) without the last term which represents the area lost by the disappearing wave. The evolution during this stage can be observed between points 3 and 4 in Figure 4.3.

Also, Figure 5.1 shows in detail the evolution of the boundary layer profile from the time that  $J > J_c$ . Initially,  $u$  grows at the injecting boundary because  $J$  increases. Furthermore, the slope  $\partial u(0, t)/\partial x$  increases and it becomes positive at a certain time. Then a wave-like structure is created. The leading front of this wave moves away from the boundary while the back-front is attached to it. The wave continues its growth until the time when  $J$  becomes again smaller than  $J_c$ . Then, the slope at the boundary becomes negative, the wave dettaches and moves away from the boundary as a solitary wave. At that time, the quasistationary part of the boundary layer which joins  $x = 0$  to the maximum at  $x = X_m$  becomes the backfront of a detached pulse. Then, we again have the same equation (2.11) describing the first stage, and a cycle of the Gunn oscillation has been completed. The time evolution during this stage can be observed in Figure 4.3 for times larger than  $t_5$ .

**6. Conclusions.** In this paper we have asymptotically described one period of a Gunn-type oscillation in a simple model. The nonlinearity of the model is such

FIG. 5.1. *Boundary layer profile evolution during the shedding stage.*

that at most two constant solutions are possible for each value of  $J$  (the current-like unknown). The model consists of a parabolic equation for the field-like unknown,  $u(x, t)$ , and an integral constraint (bias condition) which determines  $J(t)$ . Appropriate boundary and initial conditions are imposed. The key new idea of our analysis is that a pulse that changes shape as it advances may be constructed by fixing only two parameters:  $J$  and the pulse maximum,  $u_m$ . If the pulse width is small compared to the sample length,  $L$ ,  $J$  and  $u_m$  change on a slow time scale. The trailing front of the pulse is part of a separatrix joining a saddle point to  $(u_m, 0)$  with  $du/d\chi > 0$  on the  $(u, du/d\chi)$  phase plane. The initial and final points determine the backfront speed  $c_+$  as a function of  $J$  and  $u_m$ . Similarly the forefront of a pulse is constructed and its speed  $c_-$  determined. Then equations for  $J$  and  $u_m$  are obtained by time-differentiation of the bias condition and of the pulse width. The time derivative of the later is  $c_- - c_+$  and  $J$  tends towards a fixed value corresponding to a rigidly moving pulse with  $c_- = c_+$ . Other stages of a Gunn oscillation including wave creation and annihilation at the boundaries are analyzed by similar methods. Our theory compares well with direct numerical simulations.

We have found an asymptotic theory of the ‘Gunn effect’ in a simple piecewise linear model, whose main step is a construction of pulses and a derivation of an equation for the ‘current’. An analysis of the stability of these solutions is an open problem, although there is some work on this problem in the related Kroemer model [3, 25]. That the profile of pulses can become oscillatory for appropriate parameter values has been shown by Sun et al for some reaction-diffusion models [23]. We expect that the present method yield results independent of the model equations within a class thereof displaying the Gunn instability [6, 21, 22, 25, 26]. Studies of other systems that can be understood by the dynamics of pulses are in progress.

## Appendix A. Limiting cases.

**A.1. Triangular pulses.** The bias condition (2.2) determines the orders of magnitude of  $\chi_m$  and  $u_m$  in terms of the small parameter  $\epsilon$ . Let us assume that  $(K - c_+)$

and  $(J - \alpha)$  are  $O(1)$ , whereas  $\chi_m \gg 1$ . Then (3.17), (3.18) and (3.19) imply that

$$\begin{aligned} u_m &= u_M + \frac{J - \alpha}{K - c_+} \chi_m - \frac{\lambda_+(u_M - u_1)}{K - c_+} \\ &\sim \frac{J - \alpha}{K - c_+} \chi_m. \end{aligned} \quad (\text{A.1})$$

The wavefront  $u(\chi; c_+)$  is given by (3.14) for  $\chi < 0$  and

$$u = u_m + \frac{J - \alpha}{K - c_+} (\chi - \chi_m) + B_+ \left[ e^{(K - c_+)\chi} - e^{(K - c_+)\chi_m} \right] \quad (\text{A.2})$$

$$\sim \frac{J - \alpha}{K - c_+} \chi, \quad (\text{A.3})$$

for  $\chi > 0$ , where (A.1) has been used. The bias condition (2.2) then yields

$$\frac{\phi - u_1}{\epsilon} \sim \frac{J - \alpha}{K - c_+} \chi_m^2, \quad (\text{A.4})$$

$$\chi_m \sim \sqrt{\frac{(\phi - u_1)(K - c_+)}{\epsilon(J - \alpha)}}. \quad (\text{A.5})$$

These equations imply that  $\chi_m$  and  $u_m$  are  $O(\epsilon^{-\frac{1}{2}})$ , while the proper time scale over which  $J$  varies is  $t = O(\epsilon^{-\frac{1}{2}})$ .

We can obtain (A.1) - (A.5) directly from the Eq. (3.8) and the bias condition. If  $\chi_m \gg 1$ , so is  $u_m$ . Then we shall select uniquely the wavefront solution of Eq. (3.8),  $u(\chi; c_+)$ , so that it satisfies  $u(-\infty; c_+) = u_1(J)$  and it does not grow exponentially as  $\chi \rightarrow +\infty$ . Similarly,  $u(\chi; c_-) = u(-\chi; c_+)$  does not grow exponentially as  $\chi \rightarrow -\infty$ , and it satisfies  $u(+\infty; c_-) = u_1(J)$ . As in Theorem 1, we still have  $c_+ + c_- = 2K$ .

$u(\chi; c_+)$  satisfies Eq. (3.14) and

$$u(\chi; c_+) = u_M + \frac{J - \alpha}{K - c_+} \chi, \quad \text{if } \chi > 0. \quad (\text{A.6})$$

Continuity of  $du/d\chi$  at  $\chi = 0$  directly yields

$$\left( u_M - \frac{J}{\beta} \right) \lambda_+ = \frac{J - \alpha}{K - c_+},$$

which in turn implies

$$c_+ = K - \frac{J - \alpha}{\sqrt{\beta(u_M - u_1) \left( u_M - \frac{\alpha}{\beta} \right)}} > 0. \quad (\text{A.7})$$

Figure A.1 compares the actual values of  $c_{\pm}$  with the approximation (A.7). Notice that both lines are reasonably close for  $J$  sufficiently higher than  $J^*$ .

We can now form a pulse by joining the backfront  $u(\chi; c_+)$ ,  $\chi = x - X_+ < \chi_m$  to the forefront  $u(2\chi_m - \chi; c_+)$ . This pulse asymptotically approaches an isosceles triangle of basis  $(X_- - X_+) = 2\chi_m$  and height approximately given by

$$\begin{aligned} u_m &= u(\chi_m; c_+) = u\left(\frac{X_- - X_+}{2}; c_+\right) \\ &\sim \frac{(J - \alpha)(X_- - X_+)}{2(K - c_+)}. \end{aligned} \quad (\text{A.8})$$

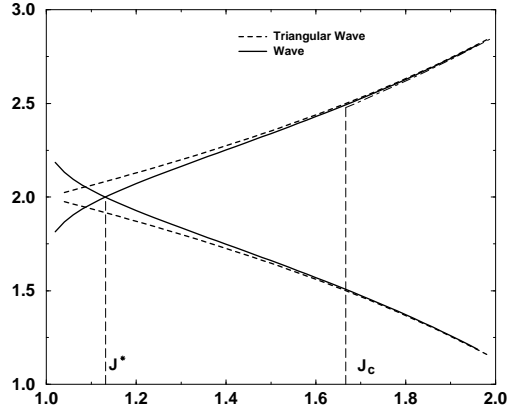


FIG. A.1. Velocities of the backfront,  $c_+$ , and of the forefront,  $c_-$ , as functions of  $J$  for  $\phi = 1.6$  and the same parameter values as in Figure 3.1. We have also shown the corresponding approximate values  $c_{\pm}$  obtained for the triangular pulse described in the text.

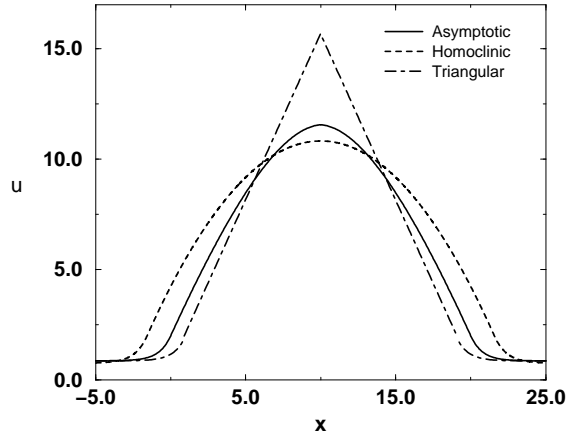


FIG. A.2. Shape of the pulse for  $J = 1.3$  and the parameter values of Figure 3.1. Also shown are the corresponding triangular and homoclinic pulses.

See Fig. A.2, which compares the triangular pulse to the real pulse and the homoclinic pulse for the same values of  $J$  and  $\phi$ . Here we have used (A.6) and assumed that  $\chi_m$  (the location of the maximum, equal to the pulse half-width) is very large. To be precise, we assume that  $(K - c_+) = O(1)$  and that  $(J - \alpha)\chi_m \gg 1$ .

Notice that the way we have constructed  $u(\chi; c_+)$  is immediately applicable to a general smooth nonlinearity  $g(u)$  of the same type. We have thus the following result:

**Result.** *Let the characteristic curve  $g(u)$  be an odd function of  $u$  with a positive local maximum after which it monotonically decays to a positive constant as  $u \rightarrow +\infty$ . The approximate backfront  $u(\chi; c_+)$  is the unique solution of Eq. (3.8) which, for an*

appropriate choice of the velocity  $c_+$ , satisfies  $u(-\infty; c_+) = u_1(J)$  and it does not grow exponentially as  $\chi \rightarrow +\infty$ .

**A.2. The homoclinic pulse.** If  $c_+ = c_- = K$ , the pulse is a homoclinic orbit of the phase plane (3.8):

$$(A.9) \quad \frac{\partial^2 u}{\partial \zeta^2} + J - g(u) = 0,$$

with  $u(\pm\infty) = u_1(J) = J/\beta$ . See Fig. 4.2. Here  $\zeta \equiv x - X_0$ , and  $X_0 = (X_+ + X_-)/2$  is the location of the maximum of the pulse,  $u_m$ . The solution is

$$(A.10) \quad u(\zeta) = \frac{J}{\beta} + \left(u_M - \frac{J}{\beta}\right) e^{-\sqrt{\beta}(|\zeta| - \zeta_0)} \quad \text{for } |\zeta| > \zeta_0,$$

$$(A.11) \quad u(\zeta) = u_m - \frac{J - \alpha}{2} \zeta^2 \quad \text{for } |\zeta| < \zeta_0,$$

$$(A.12) \quad u_m = u_M + \frac{J - \alpha}{2} \zeta_0^2.$$

$\zeta_0$  is determined by imposing continuity of  $du/d\zeta$  at  $\zeta = \pm\zeta_0$ :

$$(A.13) \quad \zeta_0 = \frac{\sqrt{\beta} \left(u_M - \frac{J}{\beta}\right)}{J - \alpha}.$$

Now we may find  $J = J^*$  from the bias condition. The result is

$$(A.14) \quad J^* = \alpha + \beta^{\frac{3}{4}} \sqrt{\frac{2\epsilon \left(u_M - \frac{\alpha}{\beta}\right)^3}{3 \left(\phi - \frac{\alpha}{\beta}\right)}} + O(\epsilon),$$

$$(A.15) \quad \zeta_0 = \beta^{-\frac{1}{4}} \sqrt{\frac{3 \left(\phi - \frac{\alpha}{\beta}\right)}{2\epsilon \left(u_M - \frac{\alpha}{\beta}\right)}} + O(1),$$

$$(A.16) \quad u_m = \frac{\beta^{\frac{1}{4}}}{2} \sqrt{\frac{3}{2\epsilon} \left(\phi - \frac{\alpha}{\beta}\right) \left(u_M - \frac{\alpha}{\beta}\right)} + O(1).$$

Fig. A.3 compares  $J^*$  to the approximation (A.14). Notice that a simple phase plane argument indicates that  $J^*$  obeys the following equal-area rule:

$$(A.17) \quad J^* = \frac{1}{u_m - u_1} \int_{u_1}^{u_m} g(u) du,$$

where  $u_m$  is given by Eq. (A.16). Fig. A.2 compares the actual pulse, the homoclinic pulse with  $c = K$  and the triangular wave for the same values of  $J$  and  $\phi$ .

**Appendix B. Explicit calculation of  $P^{(1)}$  and  $c_+^{(1)}$ .** First of all,  $P^{(1)} = P_\chi^{(0)} \equiv \partial P^{(0)}/\partial \chi$  is a solution of the homogeneous problem (4.12) (with zero right hand side) and (4.13). The solvability conditions for the nonhomogeneous problem

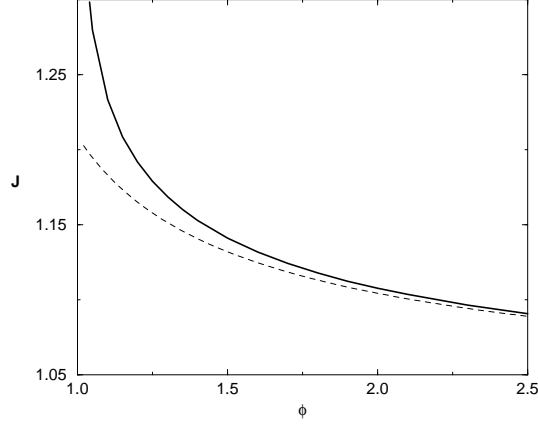


FIG. A.3. Value  $J = J^*$  for the homoclinic pulse as a function of the bias  $\phi$ . The dashed curve corresponds to the approximation (A.14).

yield

$$(B.1) \quad \begin{aligned} & \left[ P_{\chi}^{(0)} P_{\chi}^{(1)} - P_{\chi\chi}^{(0)} P^{(1)} \right]_{\chi=\chi_m} e^{-(K-c_+^{(0)})\chi_m} \\ &= \int_{-\infty}^{\chi_m} P_{\chi}^{(0)} \left[ P_s^{(0)} - J^{(1)} - c_+^{(1)} P_{\chi}^{(0)} \right] e^{-(K-c_+^{(0)})\chi} d\chi, \end{aligned}$$

$$(B.2) \quad c_+^{(1)} + c_-^{(1)} = 0.$$

Let us define

$$(B.3) \quad P^{(1)} \equiv p(\chi; c_+^{(0)}) \frac{\partial P^{(0)}}{\partial \chi}.$$

Inserting (B.3) in (4.12), we obtain an equation which can be solved by two quadratures. We find

$$(B.4) \quad \frac{\partial p}{\partial \chi} = \frac{e^{(K-c_+^{(0)})\chi}}{P_{\chi}^{(0)2}} \int_{-\infty}^{\chi} e^{-(K-c_+^{(0)})\chi} P_{\chi}^{(0)} \left[ P_s^{(0)} - J^{(1)} - c_+^{(1)} P_{\chi}^{(0)} \right] d\chi.$$

Here subscripts indicate partial derivatives with respect to the corresponding variable. It is easy to check that this expression satisfies (B.1). Further integration yields (for  $\chi < 0$ )

$$(B.5) \quad \begin{aligned} p &= \frac{(\beta J^{(1)} - J_s^{(0)}) e^{-\lambda_+ \chi}}{\beta^2 \lambda_+ (u_M - u_1)} + \frac{\lambda_{+s} \chi^2}{2\lambda_+ \sqrt{(K - c_+^{(0)})^2 + 4\beta}} \\ & - \frac{\chi}{\sqrt{(K - c_+^{(0)})^2 + 4\beta}} \left[ \frac{J_s^{(0)}}{\beta \lambda_+ (u_M - u_1)} + \frac{\lambda_{+s}}{\lambda_+ \sqrt{(K - c_+^{(0)})^2 + 4\beta}} + c_+^{(1)} \right] + q, \end{aligned}$$

where  $q$  is a constant. For  $\chi > 0$ ,  $P_{\chi\chi}^{(0)} = B_+(K - c_+^{(0)})^2 e^{(K - c_+^{(0)})\chi}$  and we can simplify the expression for  $p$  by integrating by parts. The result is

$$(B.6) \quad p = \frac{1}{B_+(K - c_+^{(0)})^2 P_\chi^{(0)}} \left\{ P_\chi^{(0)} \int_0^\chi e^{-(K - c_+^{(0)})\chi} \left[ P_s^{(0)} - J^{(1)} - c_+^{(1)} P_\chi^{(0)} \right] d\chi - \int_{-\infty}^\chi e^{-(K - c_+^{(0)})\chi} P_\chi^{(0)} \left[ P_s^{(0)} - J^{(1)} - c_+^{(1)} P_\chi^{(0)} \right] d\chi \right\} + Q.$$

Continuity of  $p$  at  $\chi = 0$  yields

$$(B.7) \quad q = Q - \frac{J^{(1)} - \frac{J_s^{(0)}}{\beta} + \frac{\beta I_0}{B_+(K - c_+^{(0)})^2}}{\lambda_+ \beta (u_M - u_1)}$$

where  $I_0$  is the following integral:

$$I_0 \equiv \int_{-\infty}^0 e^{-(K - c_+^{(0)})\chi} P_\chi^{(0)} \left[ P_s^{(0)} - J^{(1)} - c_+^{(1)} P_\chi^{(0)} \right] d\chi$$

whose value can be computed as,

$$(B.8) \quad I_0 = I_{00} + I_{0J} J^{(1)} + I_{0c} c_+^{(1)}$$

where

$$\begin{aligned} I_{00} &= \frac{\lambda_+^2 (u_M - u_1)}{\sqrt{(K - c_+^{(0)})^2 + 4\beta}} \left[ \frac{\lambda_+ J_s^{(0)}}{\beta^2} + \frac{(u_M - u_1) c_{+s}}{(K - c_+^{(0)})^2 + 4\beta} \right] \\ I_{0J} &= -\frac{\lambda_+^2 (u_M - u_1)}{\beta} \\ I_{0c} &= -\frac{\lambda_+^2 (u_M - u_1)^2}{\sqrt{(K - c_+^{(0)})^2 + 4\beta}} \end{aligned}$$

Continuity of  $P_\chi^{(1)}$  at  $\chi = 0$  implies

$$(B.9) \quad P_\chi^{(0)}(0) [p_\chi(0+) - p_\chi(0-)] = -p(0) \left[ P_{\chi\chi}^{(0)}(0+) - P_{\chi\chi}^{(0)}(0-) \right].$$

The second argument  $c_+^{(0)}$  has been omitted in all the functions in this formula. The jump discontinuity of the second derivative  $P_{\chi\chi}^{(0)}$  at  $\chi = 0$  implies that  $p_\chi$  has also a jump discontinuity at  $\chi = 0$ . Substituting (B.5) and (B.6) in (B.9), we obtain

$$(B.10) \quad \begin{aligned} QB_+(K - c_+^{(0)})^2 &= q\lambda_+^2 (u_M - u_1) - \frac{1}{\sqrt{(K - c_+^{(0)})^2 + 4\beta}} \\ &\times \left[ \frac{J_s^{(0)}}{\beta} + (u_M - u_1)\lambda_+ c_+^{(1)} + \frac{\lambda_+ s (u_M - u_1)}{\sqrt{(K - c_+^{(0)})^2 + 4\beta}} \right]. \end{aligned}$$

We can obtain  $Q$  from (B.7), (B.8) and (B.10). After some algebra, the result is

$$(B.11) \quad Q = Q_0 + Q_J J^{(1)} + Q_c c_+^{(1)}$$

with

$$\begin{aligned} v Q_0 &= \frac{J_s^{(0)}}{\beta} \left[ \frac{1}{\sqrt{(K - c_+^{(0)})^2 + 4\beta}} - \frac{\lambda_+}{\beta} \right] + \\ &\quad + \frac{\lambda_+ I_{00}}{B_+(K - c_+^{(0)})^2} - \frac{\lambda_+ (u_M - u_1) c_{+s}^{(0)}}{[(K - c_+^{(0)})^2 + 4\beta]^{3/2}} \\ v Q_J &= \frac{\lambda_+ I_{0J}}{B_+(K - c_+^{(0)})^2} + \frac{\lambda_+}{\beta} \\ v Q_c &= \frac{\lambda_+ I_{0c}}{B_+(K - c_+^{(0)})^2} + \frac{\lambda_+ (u_M - u_1)}{\sqrt{(K - c_+^{(0)})^2 + 4\beta}} \\ v &= \lambda_+^2 (u_M - u_1) - B_+(K - c_+^{(0)})^2 \end{aligned}$$

The velocity correction  $c_+^{(1)}$  can be obtained from the condition  $\partial P^{(1)}/\partial \chi = 0$  at  $\chi = \chi_m$ . Thus

$$(B.12) \quad \begin{aligned} Q &+ \frac{1}{B_+(K - c_+^{(0)})^2} \int_0^{\chi_m} e^{-(K - c_+^{(0)})\chi} P_\chi^{(0)} \\ &\times [P_s^{(0)} - J^{(1)} - c_+^{(1)} P_\chi^{(0)}] d\chi = 0. \end{aligned}$$

Inserting (B.11) in this equation, we get  $c_+^{(1)}$ . After simplification, the result is

$$(B.13) \quad \gamma c_+^{(1)} = c_{+0} + c_{+J} J_c^{(1)}$$

with

$$\begin{aligned} c_{+0} &= \frac{J_s^{(0)}}{K - c_+^{(0)}} \left[ z_1 + \frac{z_2}{K - c_+^{(0)}} + (\chi_m + z_2) \left( \frac{\lambda_+}{\beta} + \frac{1}{K - c_+^{(0)}} \right) \right] \\ &+ \frac{c_{+s}^{(0)}}{(K - c_+^{(0)})^2} \left[ 2(\chi_m + z_2) \left( \frac{J^{(0)} - \alpha}{K - c_+^{(0)}} - \frac{\beta(u_M - u_1)}{\sqrt{(K - c_+^{(0)})^2 + 4\beta}} \right) \right. \\ &\quad \left. + (J^{(0)} - \alpha) \left( z_1 + \frac{z_2}{K - c_+^{(0)}} \right) - \frac{B_+}{2} (K - c_+^{(0)})^2 \chi_m^2 \right] \\ &\quad - B_+ Q_0 (K - c_+^{(0)})^2 \\ c_{+J} &= -z_2 - B_+ Q_J (K - c_+^{(0)})^2 \\ \gamma &= \frac{J^{(0)} - \alpha}{K - c_+^{(0)}} z_2 - B_+ (K - c_+^{(0)}) \chi_m + B_+ Q_c (K - c_+^{(0)})^2 \\ z_1 &\equiv \frac{\chi_m \exp[(K - c_+^{(0)})\chi_m]}{(K - c_+^{(0)})} = -\frac{\chi_m B_+ (K - c_+^{(0)})}{J^{(0)} - \alpha} \\ z_2 &\equiv \frac{\exp[(K - c_+^{(0)})\chi_m] - 1}{(K - c_+^{(0)})} = -\frac{\lambda_+ (u_M - u_1)}{J^{(0)} - \alpha} \end{aligned}$$



Here we have used (3.16) - (3.18) to simplify the result.  $J^{(1)}$  is found from the equation:

$$(B.14) \quad \begin{aligned} 0 = & 2 \int_{-\infty}^0 (P^{(0)} - u_1) d\chi + \frac{J^{(1)} - g_1' J_s^{(0)}}{g_1'^2} \\ & + 2\epsilon \int_0^{\chi_m} P^{(1)} d\chi + \int_0^\infty (U_L(\xi) - u_1) d\xi \\ & + \int_0^\infty (U_R(\xi) - u_1) d\xi, \end{aligned}$$

after substitution of (4.14), (4.15) and (B.13).

### Appendix C. Pulse Dynamics: Limiting cases.

**C.1. Triangular pulse.** If the limiting pulse is triangular, the approximate evolution equation for  $J$  may be obtained by time-differentiating (A.5) and using (A.7):

$$(C.1) \quad \frac{dJ}{dt} = -\sqrt{\epsilon} B(J) [K - c_+(J)],$$

$$(C.2) \quad B(J) = \frac{4\beta(\beta u_M - \alpha)^{\frac{1}{4}}(\phi - u_1)^{\frac{1}{2}}(u_M - u_1)^{\frac{5}{4}}}{2u_M - \phi - u_1}.$$

For typical values of the parameters such as those in Fig. 3.1,  $B(J) > 0$ , so that  $J$  tends to the solution of  $c_+(J) = K$ . Triangular pulses are good approximations for  $J$  sufficiently large, which means that the solution of (C.1) decreases towards  $J = \alpha$  according to (A.7). Of course before this value can be reached, (C.1) ceases to be valid and we revert to the general equation for  $J$ , (2.11), whose fixed point is  $J^*$ .

**C.2. Homoclinic pulse.** Let us now assume that  $(K - c_+) \ll (J - \alpha) \ll 1$ , whereas  $\chi_m \gg 1$ . Then (3.17) and (3.18) imply that

$$(C.3) \quad \chi_m \sim \frac{\lambda_+(u_M - u_1)}{J - \alpha} + \frac{\lambda_+^2(u_M - u_1)^2(K - c_+)}{2(J - \alpha)^2}.$$

Here  $\lambda_+ \sim \sqrt{\beta}$ . Notice that (C.3) becomes (A.13) as  $(K - c_+) \rightarrow 0$ . We now insert this approximation in (3.19) after (3.17) has been substituted. The result is

$$(C.4) \quad u_m \sim u_M + \frac{\lambda_+^2(u_M - u_1)^2}{2(J - \alpha)} \sim \frac{1}{2}(J - \alpha)\chi_m^2.$$

The bias condition (4.15) may now be approximated by using (C.3) and (C.4) to obtain

$$\frac{\phi - u_1}{\epsilon} \sim \frac{2\beta^{\frac{3}{2}}(u_M - u_1)^3}{3(J - \alpha)^2}.$$

Then

$$(C.5) \quad \begin{aligned} (J - \alpha) & \sim \beta^{\frac{3}{4}} \sqrt{\frac{2\epsilon(u_M - u_1)^3}{3(\phi - u_1)}} \\ & \sim \beta^{\frac{3}{4}} \sqrt{\frac{2\epsilon\left(u_M - \frac{\alpha}{\beta}\right)^3}{3\left(\phi - \frac{\alpha}{\beta}\right)}}. \end{aligned}$$

Inserting (C.5) in (C.3) and (C.4), we obtain

$$(C.6) \quad \chi_m \sim \beta^{-\frac{1}{4}} \sqrt{\frac{3(\phi - u_1)}{2\epsilon(u_M - u_1)}},$$

$$(C.7) \quad u_m \sim \frac{\beta^{\frac{1}{4}}}{2} \sqrt{\frac{3}{2\epsilon} (\phi - u_1)(u_M - u_1)}.$$

Equations (C.5) - (C.7) are the same as (A.14) - (A.16) for the homoclinic pulse.

As explained before,  $d\chi_m/dt = (c_- - c_+)/2 = K - c_+$ . Therefore the derivative of (C.6) with respect to time yield

$$(C.8) \quad \frac{dJ}{dt} \sim -\sqrt{\frac{8\epsilon}{3}} \frac{\beta^{\frac{5}{4}} (\phi - u_1)^{\frac{1}{2}} (u_M - u_1)^{\frac{3}{2}}}{u_M - \phi} (K - c_+).$$

This equation has the same form as (2.11), and it shows that the unknown  $J(t)$  varies on a slow time scale  $t = O(1/\sqrt{\epsilon(K - c_+)})$ . In the present limit,  $(K - c_+) \ll (J - \alpha) = O(\sqrt{\epsilon})$ , so that the corresponding time scale is slower than  $\tau = \epsilon t$ .

A glance to Eq. (C.8) shows that  $J$  decreases exponentially fast to  $J^*$  such that  $c_+ = c_- = K$ . The resulting pulse is the homoclinic orbit of the phase plane (3.8) with  $c = K$  described in the previous Section.

#### REFERENCES

- [1] V. L. BONCH-BRUEVICH, I. P. ZVYAGIN, AND A. G. MIRONOV, *Domain electrical instabilities in semiconductors*, (Consultants Bureau, 1975, New York).
- [2] L. L. BONILLA, *Solitary waves in semiconductors with finite geometry and the Gunn effect*. SIAM J. Appl. Math. **51** (1991), pp. 727-747.
- [3] L.L. BONILLA, F. HIGUERA AND S. VENAKIDES, *The Gunn effect: Instability of the steady state and stability of the solitary wave in long extrinsic semiconductors*. SIAM J. Appl. Math. **54** (1994), pp. 1521-1541.
- [4] L. L. BONILLA AND F. J. HIGUERA, *The Onset and End of the Gunn Effect in Extrinsic Semiconductors*. SIAM J. Appl. Math. **55** (1995), pp. 1625-1649.
- [5] L. L. BONILLA, I. R. CANTALAPIEDRA, G. GOMILA AND J. M. RUBÍ, *Asymptotic analysis of the Gunn effect with realistic boundary conditions*. Phys. Rev. E **56** (1997), pp. 1500-1510.
- [6] L. L. BONILLA AND I. R. CANTALAPIEDRA, *Universality of the Gunn effect: self-sustained oscillations mediated by solitary waves*. Phys. Rev. E **56** (1997), pp. 3628-3632.
- [7] L. L. BONILLA, A. L. SÁNCHEZ AND M. CARRETERO, *The description of homogeneous branched-chain explosions with slow radical recombination by self-adjusting time scales*. SIAM J. Appl. Math. **61** (2000), pp. 528-550.
- [8] L. L. BONILLA, *Theory of Nonlinear Charge Transport, Wave Propagation and Self-oscillations in Semiconductor Superlattices*. J. Phys. Cond. Matter **14** (2002), pp. R341-R381.
- [9] A. E. BUGRIM, A.M. ZHABOTINSKY AND I.R. EPSTEIN, *Calcium Waves in a Model with a Random Spatially Discrete Distribution of Ca2+ Release Sites*. Biophys. J. **73** (1997), pp. 2897-2906.
- [10] P. N. BUTCHER, W. FAWCETT, AND C. HILSUM, *A simple analysis of stable domain propagation in the Gunn effect*. Brit. J. Appl. Phys. **17** (1966), pp. 841-850.
- [11] M. BÜTTIKER AND H. THOMAS, *Current instability and domain propagation due to Bragg scattering*. Phys. Rev. Lett. **38** (1977), pp. 78-80.
- [12] A. DOELMAN, W. ECKHAUS AND T. J. KAPER, *Slowly Modulated Two-Pulse Solutions in the Gray-Scott Model I: Asymptotic construction and Stability*. SIAM J. Appl. Math. **61** (2000), pp. 1080-1102.
- [13] H. HEMPEL, I. SCHEBESCH AND L. SCHIMANSKY-GEIER, *Traveling pulses in reaction-diffusion systems under global constraints*. Eur. Phys. J. B **2** (1998), pp. 399-407.
- [14] F. J. HIGUERA AND L. L. BONILLA, *Gunn instability in finite samples of GaAs. II Oscillatory states in long samples*. Physica D **57** (1992), pp. 161-184.

- [15] K. HOFBECK, J. GRENZER, E. SCHOMBURG, A. A. IGNATOV, K. F. RENK, D. G. PAVEL'EV, YU. KOSCHURINOV, B. MELZER, S. IVANOV, S. SCHAPOSHNIKOV AND P. S. KOP'EV, *High-frequency self-sustained current oscillation in an Esaki-Tsu superlattice monitored via microwave emission*. Phys. Lett. A **218** (1996), pp. 349-353.
- [16] D. IRON AND M. WARD, *A metastable spike solution for a nonlocal RD model*. SIAM J. Appl. Math. **60** (2000), pp. 778-802.
- [17] J. P. KEENER, *Propagation and its failure in coupled systems of discrete excitable cells*. SIAM J. Appl. Math. **47** (1987), pp. 556-572.
- [18] J.P. KEENER AND J. SNEYD, *Mathematical Physiology* (Springer, New York, 1998). Chapter 9.
- [19] J. LIANG, *On a nonlinear integrodifferential semiconductor model*. SIAM J. Math. Anal. **25** (1994), pp. 1375-1392.
- [20] J. RINZEL AND J. B. KELLER, *Traveling waves solutions of a nerve conduction equation*. Biophys. J. **13** (1973), pp. 1313-1337.
- [21] V. A. SAMUILOV, *Nonlinear and chaotic charge transport in semi-insulating semiconductors*, in *Nonlinear Dynamics and Pattern Formation in Semiconductors and Devices*, edited by F.-J. Niedernostheide (Springer Verlag, 1995, Berlin), pp. 220-249.
- [22] M. P. SHAW, H. L. GRUBIN AND P. R. SOLOMON, *The Gunn-Hilsum effect*. Academic Press, 1979, New York).
- [23] W. SUN, T. TANG, M.J. WARD AND J. WEI, *Numerical Challenges for Resolving Spike Dynamics for Two Reaction-Diffusion Systems*. Studies in Applied Math, **111** (2003), pp. 41-84.
- [24] S. W. TEITSWORTH, *The physics of space charge instabilities and temporal chaos in extrinsic semiconductors*. Appl. Phys. A **48** (1989), pp. 127-136.
- [25] A. F. VOLKOV AND SH. M. KOGAN, *Physical phenomena in semiconductors with negative differential conductivity*. Sov. Phys. Usp. **11** (1969), pp. 881-903. [Usp. Fiz. Nauk. **96** (1968), pp. 633-672].
- [26] A. WACKER, *Semiconductor superlattices: A model system for nonlinear transport*, Phys. Rep. **357** (2002), pp. 1-111.